

# Proton conductivity and chemical stability of $\text{Li}_2\text{SO}_4$ based electrolyte in a $\text{H}_2\text{S}$ –air fuel cell

Jinxia Li, Jing-Li Luo\*, Karl T. Chuang, Alan R. Sanger

*Department of Chemical and Materials Engineering, University of Alberta, Edmonton, Alta., Canada T6G 2G6*

Received 5 January 2006; received in revised form 11 February 2006; accepted 13 February 2006

Available online 29 March 2006

## Abstract

Proton conductivity of  $\text{Li}_2\text{SO}_4\text{-Al}_2\text{O}_3$  (LA) based electrolyte was determined under non-reducing dynamic conditions using current interruption technique. The performance of LA as electrolyte has been examined at  $600^\circ\text{C}$  in a  $\text{H}_2\text{S}$  fuel cell with  $\text{MoS}_2\text{-NiS}$  as anode catalyst and  $\text{NiO}$  as cathode catalyst. XRD and XPS results show that  $\text{Li}_2\text{SO}_4$  is not stable when heated in pure  $\text{H}_2\text{S}$  as it is reduced to  $\text{Li}_2\text{S}$  by hydrogen produced in equilibrium amounts from the thermal decomposition of  $\text{H}_2\text{S}$ . In contrast, under dynamic operation in a  $\text{H}_2\text{S}$  fuel cell the concentration of  $\text{H}_2$  is much lower, the reduction reaction does not occur and, surprisingly,  $\text{Li}_2\text{SO}_4$  is a chemically stable electrolyte.

© 2006 Published by Elsevier B.V.

**Keywords:** Proton conductivity; Chemical stability; Lithium sulfate; Intermediate temperature; Fuel cells

## 1. Introduction

Oxidation of hydrogen sulfide ( $\text{H}_2\text{S}$ ) to elemental sulfur is highly exothermic.  $\text{H}_2\text{S}$  occurs naturally in natural gas (from a few ppm to over 80%), volcanic gases, some hot springs and crude petroleum. However,  $\text{H}_2\text{S}$  is highly toxic even at low concentrations. It is also highly flammable, forming an explosive mixture with air over a wide range of concentrations (4.3–46%). The most important industrial use of hydrogen sulfide is as a source of about 25% of the world production of elemental sulphur. The Claus manufacturing process is based on oxidizing about 1/3 of  $\text{H}_2\text{S}$  to  $\text{SO}_2$ , then reacting the resulting  $\text{SO}_2$  with the remaining  $\text{H}_2\text{S}$  to form sulfur and steam over a catalyst.

Presently, the energy generated in the Claus process is either vented or recovered as low grade thermal energy. So it is economically and environmentally desirable to recover this energy more efficiently, and preferably as high-grade electrical power. It has long been recognized that  $\text{H}_2\text{S}$  is a potentially valuable fuel for a fuel cell. Many groups have investigated high temperature  $\text{H}_2\text{S}\text{-O}_2$  solid oxide fuel cells (SOFC) using yttria or calcia stabilized zirconia as the electrolyte

[1–3]. However, the electrolytes used were oxygen ion conductors and the operating temperatures were high. The thermodynamics of the reaction make it desirable to use an electrolyte with high conductivity capable of use at intermediate temperatures.

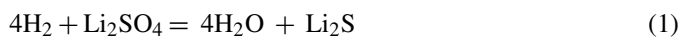
It has been established that protons can be mobile at high temperatures in some oxide materials [4,5]. Also, it is found that proton conductors may have much higher ionic conductivities than oxygen conductors at the same high temperature. Since then, a number of studies have been carried out on proton conduction in various alkaline earth perovskite-type oxide ceramics doped with rare earth oxides [6–9].

$\alpha\text{-Li}_2\text{SO}_4$  is stable between the melting point at  $860^\circ\text{C}$  and the first-order phase transition at  $575^\circ\text{C}$ , below which the crystal structure transforms to the low-temperature monoclinic  $\beta$ -phase [10]. The  $\alpha$ -phase is cubic; the sulphate groups occupy the (0, 0, 0) position in a face-centered cubic cell (space group:  $Fm\bar{3}m$ ), and have a high degree of rotational freedom [11]. Some high temperature sulfate phases can equally well be considered as plastic crystals (rotator phases) or as solid electrolytes (superionic conductors) [12].  $\text{Li}_2\text{SO}_4$  is an excellent lithium ion conductor in the high temperature  $\alpha$ -phase, but it is also a proton conductor in a hydrogen-containing atmosphere.  $\text{Li}_2\text{SO}_4$  is a good proton conductor at intermediate temperatures ( $600\text{--}850^\circ\text{C}$ ) and so its structural and electrical properties have been intensively researched [13,14].

\* Corresponding author. Tel.: +1 780 492 2232; fax: +1 780 492 2881.  
E-mail address: [jingli.luo@ualberta.ca](mailto:jingli.luo@ualberta.ca) (J.-L. Luo).

Since the discovery of proton conduction in  $\text{Li}_2\text{SO}_4$  [15], wide investigations have been made into both fundamental and applied aspects of its proton conductivity, especially potential applications for use in intermediate temperature fuel cells. During fuel cell operation, and especially at moderate temperatures, water is generated mainly at the cathode, showing that the electrolyte is a proton conductor rather than an oxide ion conductor.

However, it has been found that  $\text{Li}_2\text{SO}_4$  is inherently chemically unstable in the reducing  $\text{H}_2$  atmosphere under  $\text{H}_2/\text{O}_2$  fuel cell operation, and it is reduced to  $\text{Li}_2\text{S}$  and  $\text{LiOH}$  (Eqs. (1) and (2)) with consequent degradation of fuel cell performance [14].



In contrast to use of  $\text{H}_2$  as fuel,  $\text{Li}_2\text{SO}_4$  electrolyte appeared to be chemically stable under the operation conditions of a fuel cell using  $\text{H}_2\text{S}$  as the fuel [16].

Managing sulfur in the feed and product streams is a significant problem for operation of all current SOFC, PEFC and MCFC fuel cell technologies. When sulfur is present in the feed of many current systems both the performance and lifetime of the fuel cells are significantly decreased. Removal of all sulfur in the feed requires expensive gas treatment systems. Thus it is desirable to use high performance electrolytes and electrode catalysts that are stable in the presence of sulfur and its compounds. Theoretically, sulfate-based electrolytes are chemically resistant to  $\text{H}_2\text{S}$  and any sulfur containing feed gases, such as natural gas. Therefore, sulfate-based fuel cells are prospective candidates for direct use of sulfur containing fuels, thus avoiding the gas pre-treatment step for removal of sulfur, eliminating the problems with the presence of intrinsic sulfur for all fuel cell systems. A highly sulfur-tolerant fuel cell system would be able to efficiently utilize fuels based on natural gas, coal gas and landfill gas without a high pretreatment cost imposed by a traditional clean-up system.

Experimental data for  $\text{H}_2\text{S}/\text{O}_2$  fuel cells using  $\text{Li}_2\text{SO}_4$ -based electrolytes were in agreement with theoretical predictions that  $\text{Li}_2\text{SO}_4\text{-Al}_2\text{O}_3$  fuel cells are chemically stable under operation with  $\text{H}_2\text{S}$  fuel [16]. In addition, it is of interest that lithium sulphate can be exposed to moist air for a long time at high temperature without any visible changes. For these reasons, this salt has been among the most intensively studied protonic electrolytes [15].

However, it is well known that  $\text{H}_2\text{S}$  will decompose to hydrogen and sulfur at such a high temperature ( $T \geq 600^\circ\text{C}$ ) via the general equilibrium [17]:



It was unknown whether  $\text{Li}_2\text{SO}_4$  would be stable in this equilibrium mixture atmosphere. Furthermore, preliminary data showed performance of fuel cells using this electrolyte were not as good as expected based on reported high conductivity values for  $\text{Li}_2\text{SO}_4$  as electrolyte [16]. We have now resolved these questions.

Composite solid electrolytes are a new class of ion conducting materials that are of value for their mechanical and transport

properties. They can be considerably improved by variation of morphology, chemical nature and concentration of an inert additive. A common way to improve the ionic conductivity of at least moderately conducting solid electrolytes is to mix the ion conducting material with finely grained aluminum oxide to form a two-phase composite system. The presence of alumina may also improve the mechanical properties of the electrolyte. Composite solid electrolytes thus obtained give fairly reproducible values of conductivity which depend only on the  $\gamma\text{-Al}_2\text{O}_3$  content of  $[(1-x)\text{Li}_2\text{SO}_4 - x\text{Al}_2\text{O}_3]$  composites ( $x$  is the proportion of  $\text{Al}_2\text{O}_3$  by weight). It should be noted that their mechanical properties differ markedly from those of pure  $\text{Li}_2\text{SO}_4$ . No cracks in composites having  $x \geq 0.5$  have been observed and pellets have high resistance to strains and breaks [18].

Consequently, we have now determined the proton conductivity of  $\text{Li}_2\text{SO}_4\text{-Al}_2\text{O}_3$  electrolyte and the stability of  $\text{Li}_2\text{SO}_4$  under different conditions in pure  $\text{H}_2\text{S}$ .

## 2. Experimental

All chemicals used in this work were obtained from Alfa-Aesar, except as otherwise indicated.

### 2.1. Preparation of membranes

To prepare an electrolyte membrane with a designed composition, the appropriate amount of  $\text{Li}_2\text{SO}_4$  was weighed and dissolved in a minimum amount of water. The complementary amount of  $\text{Al}_2\text{O}_3$  was added and the mixture then was mixed well to form a paste. The weight ratio of  $\text{Li}_2\text{SO}_4$  to  $\text{Al}_2\text{O}_3$  was normally selected to be 3:1 ( $x$  is 0.25). No significant advantage was found from use of alternative ratios.

The paste was dried in air, then ground to form a well-mixed powder, until the particle size was smaller than  $75\ \mu\text{m}$ . This powder ( $\sim 1\text{--}1.5\ \text{g}$ ) was then weighed and placed in a 1 in. die. It was compressed for ca. 1 h under 30 t pressure to form a wafer. The wafer so obtained was then put in an oven and heated first at  $110^\circ\text{C}$  for 30–60 min and then at  $800^\circ\text{C}$  for ca. 6 h in air.

### 2.2. Stability of LA pellets in pure $\text{H}_2\text{S}$ atmosphere and fuel cell mode

We evaluated the stability of  $\text{Li}_2\text{SO}_4$  in the LA membranes by comparing XPS of fresh membranes with those treated under  $\text{H}_2\text{S}$ –air fuel cell operating conditions for 5 h at  $600^\circ\text{C}$ . In addition, a membrane comprising the electrolyte alone, without electrodes, was heated to  $600^\circ\text{C}$  in pure  $\text{H}_2\text{S}$  for 5 h, and XRD and XPS of the fresh and treated samples were compared.

### 2.3. Preparation of electrolyte supported fuel cell membrane assemblies

The fuel cell membranes were constructed by directly screen-painting the anode and cathode layer on the two surfaces of  $\text{Li}_2\text{SO}_4\text{-Al}_2\text{O}_3$  (LA) pellets separately, the assembly then was heated in air at  $750^\circ\text{C}$  for 30 min, and then the membrane was slowly cooled to room temperature. The anode materials used

were Pt or a Ni-Mo-S composite catalyst. The cathode was Pt or NiO. Pt was applied as Pt paste (Heraeus CL11-5100). The Mo-Ni-S-based composite anode contained 95 wt% ( $\text{MoS}_2 + \text{NiS}$ , 1:1, w/w) and 5 wt% Ag [19,20].

To prepare the electrolyte/electrode unit (1 in. diameter) for installation into a cell, first the cathode side of the unit was attached with ceramic sealant (Aremco 503) to a supporting annular alumina disk 3.2 cm in diameter and 0.3 cm in thickness. An opening 1.1 cm in diameter in the center of the supporting ceramic disk allowed air to access the cathode. The combination so made was then sealed between alumina tubes. Platinum meshes were used as current collectors. The surface of the Pt mesh was refreshed in the flame of a gas lamp before each new experiment to remove any deposits that might have formed during previous tests.

The cell was heated in a tubular furnace (Thermolyne F79300) with nitrogen passing through the anode chamber and air through the cathode chamber. To cure the sealant (Aremco 503), the furnace temperature was increased at  $0.8^\circ\text{C min}^{-1}$  to  $230^\circ\text{C}$ , and held at that temperature for 1 h. The temperature then was increased to operating temperature and held at that temperature to condition the electrolyte/electrode unit.

The cell electrolyte was approximately 0.6 mm thick. Fuel cells had the following configuration:

- (i) for conductivity determinations: ( $\text{H}_2\text{S}$  chamber) Pt anode/LA/Pt (air chamber);
- (ii) for fuel cell performance testing: ( $\text{H}_2\text{S}$  chamber) Mo-Ni-S composite anode/LA/NiO (air chamber).

#### 2.4. Determination of conductivity of LA electrolyte and performance of $\text{H}_2\text{S}$ -air fuel cells

Both the conductivity and fuel cell performance were determined using pure  $\text{H}_2\text{S}$  as the anode feed. The cell open circuit voltage (OCV) was monitored as a function of time on stream. Data were recorded with a Gamry electrochemical measurement system (PC4-750). Initial electrical performance data were evaluated to determine cell integrity. Typically, a cell that had no leaks showed a steady OCV value about 30 min after switching the anode feed from nitrogen to  $\text{H}_2\text{S}$ . After a steady OCV was achieved, EIS measurements and current interruption technique were performed to determine cell resistance. In EIS measurements, the frequency region was 0.1–100,000 Hz and a stimulating ac signal of 5 mV was imposed under OCV conditions. Potentiodynamic measurements were conducted to determine the cell current-voltage performance in the IR compensation mode using the Gamry system at a scanning rate of  $1\text{ mV s}^{-1}$ .

### 3. Results and discussion

#### 3.1. Chemical stability of $\text{Li}_2\text{SO}_4$

It was known that  $\text{Li}_2\text{SO}_4$  is reduced to  $\text{Li}_2\text{S}$  and  $\text{LiOH}$  in  $\text{H}_2$  [12]. We confirmed experimentally that  $\text{Li}_2\text{SO}_4$  in our pellets prepared from LA was also reduced by  $\text{H}_2$  to  $\text{Li}_2\text{S}$  in a similar manner to reported systems.

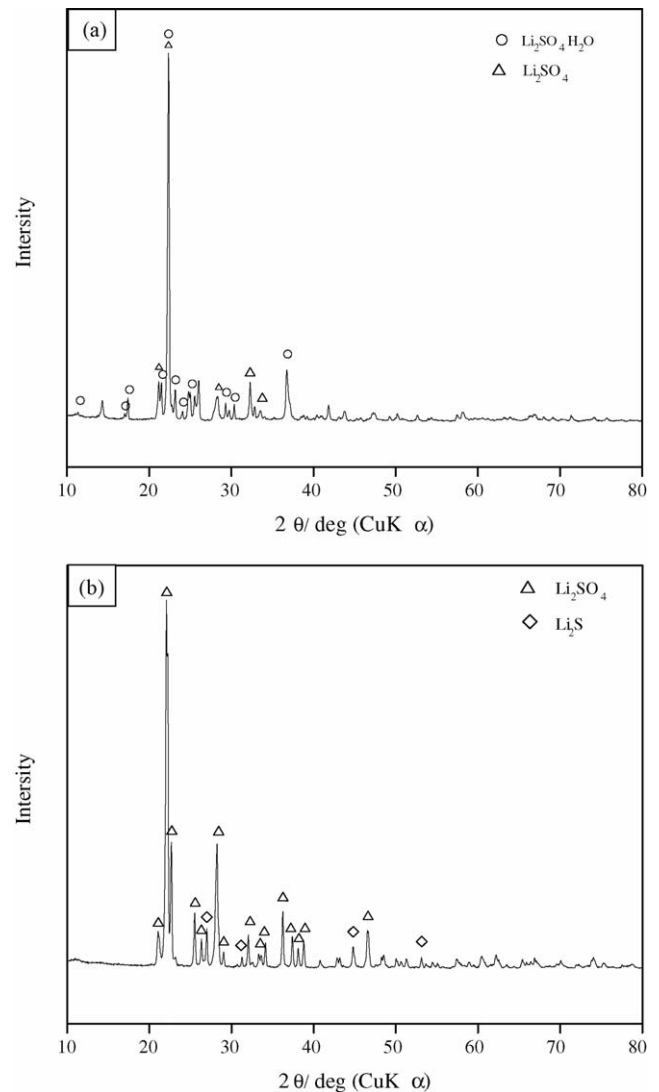
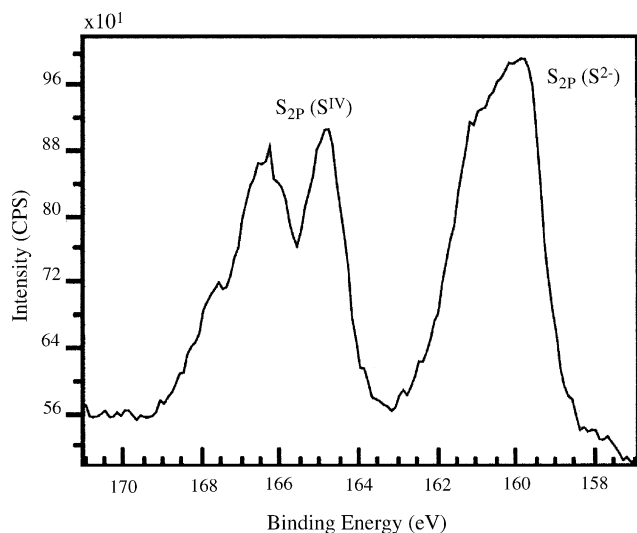


Fig. 1. XRD of  $\text{Li}_2\text{SO}_4$  (a) before and (b) after calcination in pure  $\text{H}_2\text{S}$ .

Thermodynamic calculations indicated that  $\text{Li}_2\text{SO}_4$  would not be reduced under pure  $\text{H}_2\text{S}$  [16]. However, there was no prior experimental evidence concerning the stability of  $\text{Li}_2\text{SO}_4$ - $\text{Al}_2\text{O}_3$  composites in  $\text{H}_2\text{S}$ , and so appropriate tests were performed. After being calcined in  $600^\circ\text{C}$  under  $\text{H}_2\text{S}$  for ca. 7 h, the color of the surface of  $\text{Li}_2\text{SO}_4$  pellets turned from white to brown. Fig. 1a and b show the XRD of  $\text{Li}_2\text{SO}_4$  before and after calcination in  $\text{H}_2\text{S}$ , respectively, and Fig. 2 shows the XPS of the heat treated sample. Peaks for  $\text{Li}_2\text{S}$  were found in the XRD (Fig. 1b) and XPS (Fig. 2; binding energy of  $\text{S}_{2p}$  at ca. 160 eV) of calcined samples, showing that  $\text{Li}_2\text{SO}_4$  was partly reduced.

Fig. 3 shows the equilibrium composition of the mixtures of  $\text{H}_2$ ,  $\text{S}_2$  and  $\text{H}_2\text{S}$  formed at different temperatures via reaction (3). The equilibrium concentration of  $\text{H}_2$  is approximately 2% at the fuel cell operating temperature ( $600^\circ\text{C}$ ). Reduction of  $\text{Li}_2\text{SO}_4$  to  $\text{Li}_2\text{S}$  showed that the electrolyte had reacted with  $\text{H}_2$  produced by pyrolysis of  $\text{H}_2\text{S}$ .

In contrast, no equivalent peaks were detected in samples after use under dynamic conditions during fuel cell testing. This showed that during fuel cell operation any  $\text{H}_2$  produced

Fig. 2. XPS of treated  $\text{Li}_2\text{SO}_4$ .

by pyrolysis of  $\text{H}_2\text{S}$  was rapidly consumed by electrochemical conversion to protons (Eq. (4)). Thus the concentration of  $\text{H}_2$  at the surface of the electrolyte never attained a significant value and there was no reduction of  $\text{Li}_2\text{SO}_4$ .

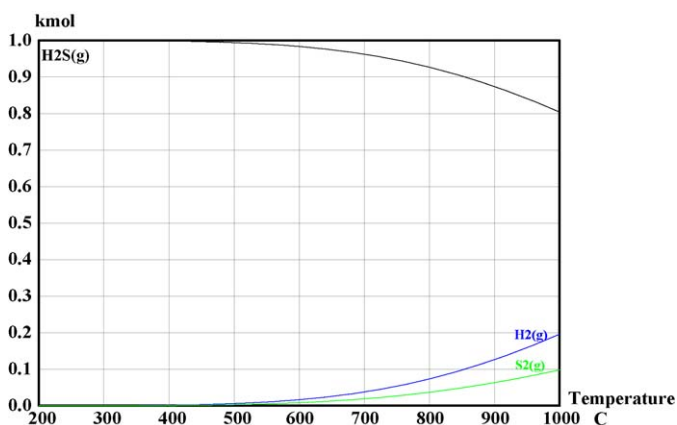
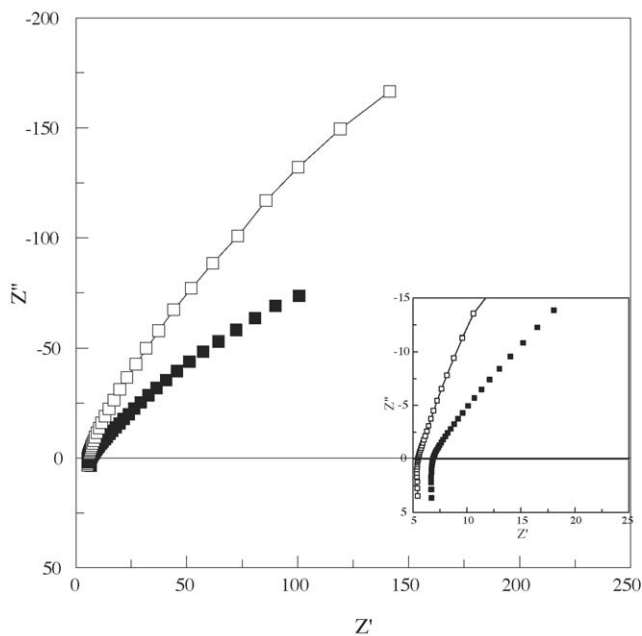


### 3.2. Membrane conductivity

The conductivity of  $\text{Li}_2\text{SO}_4$  was determined under dynamic conditions in an electrochemical cell, under which conditions it was not reduced.

It has been demonstrated through electromigration experiments with cubic lithium sulfate that the electronic conductivity is negligible in comparison with the ionic conductivity, and this was confirmed by means of conductivity measurements with blocking electrodes [21].

For the  $\text{Li}_2\text{SO}_4\text{-Al}_2\text{O}_3$  electrolyte membrane no measurable EMF was obtained in oxygen concentration cells over a wide temperature range. However, there was always an EMF response for different partial pressures of hydrogen. Thus this material

Fig. 3. Equilibrium composition of  $\text{H}_2$ ,  $\text{S}_2$  and  $\text{H}_2\text{S}$  mixtures at different temperatures.Fig. 4. Impedance of LA pellet at  $600^\circ\text{C}$  with (a)  $\text{N}_2$  and (b)  $\text{H}_2\text{S}$  in anode chamber using Pt as both anode and cathode.

was a proton conductor and had no significant oxygen ion conductivity.

Fig. 4a and b show the impedance of LA pellet at  $600^\circ\text{C}$  when the anode chamber feed was  $\text{N}_2$  and  $\text{H}_2\text{S}$ , respectively. The resistances of LA pellet were ca. 6.88 and  $5.48 \Omega$  under the respective atmospheres, and the corresponding conductivities were 0.0384 and  $0.0482 \text{ S cm}^{-1}$ . These values were very similar to the impedance values when the LA pellet was in an inert atmosphere or a  $\text{H}_2$  containing atmosphere. Thus the value obtained via ac-impedance method corresponds to the total ion conductivity rather than the proton conductivity of LA pellet.

The protonic contribution to conductivity was determined by measuring electrochemical performance with  $\text{H}_2\text{S}$  as the anode feed, as follows.

The two in situ methods commonly used for measuring ohmic losses in electrochemical cells are the current interruption method and ac impedance spectroscopy [22]. Current interruption technique [23] was used to obtain the ohmic resistances of pellets. The basic principle of the current interruption method is to interrupt the current and to observe the resulting voltage transient. The ohmic part of the overpotentials is separated from the electrochemical losses by taking advantage of the fact that the ohmic losses vanish faster than the electrochemical overpotentials when the current is interrupted.

The ohmic loss was the difference between the voltages immediately before and after the current interruption. Fig. 5 shows a typical voltage versus time trace immediately following current interruption. The sharp change in voltage corresponds to the ohmic loss and the slow change corresponds to non-ohmic polarization losses (activation and concentration). Care was taken to ensure the attainment of steady state before the current was interrupted. The proton conductivity of LA electrolyte

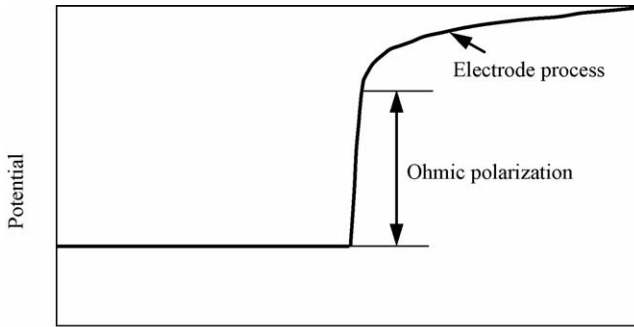


Fig. 5. Oscilloscope trace illustrating the time dependence of the electric potential before and after current interruption.

in the fuel cell was then calculated from the ohmic loss obtained from the current interruption method.

### 3.3. Fuel cell performance

Fig. 6 shows the OCV of a  $\text{H}_2\text{S}$  fuel cell which had no obvious unsteadiness or fluctuations with time, showing that the membrane was stable and did not allow gas to cross over. In contrast, OCV of porous membranes fluctuated significantly and no stable OCV value could be obtained. Membranes that had no leaks showed a steady OCV value after about 30 min. Usually, the  $\text{H}_2\text{S}$  fuel cell voltage (OCV) was less than 0.8 V, in accord with thermodynamics of the electrode reactions.  $\text{H}_2\text{S}$  dissociates at higher temperatures to form an equilibrium mixture with hydrogen and sulfur (Eq. (3)). The rate of dissociation is promoted in the presence of a suitable catalyst [3]. It can be seen from Fig. 6 that OCV of the  $\text{H}_2\text{S}$  fuel cell increased with time. As no current was drawn under OCV conditions,  $\text{H}_2$  was formed at the anode and the OCV measured comprised the sum of OCV arising from the presence of both  $\text{H}_2\text{S}$  and  $\text{H}_2$ .

Fig. 7 shows the electrochemical performance of  $\text{H}_2\text{S}$  fuel cell using  $\text{MoS}_2\text{-NiS-Ag}$  composite material as anode and NiO as cathode. The maximum current densities and power densities achieved were  $80 \text{ mA cm}^{-2}$  and  $56 \text{ mW cm}^{-2}$  using the optimum compositions of materials.

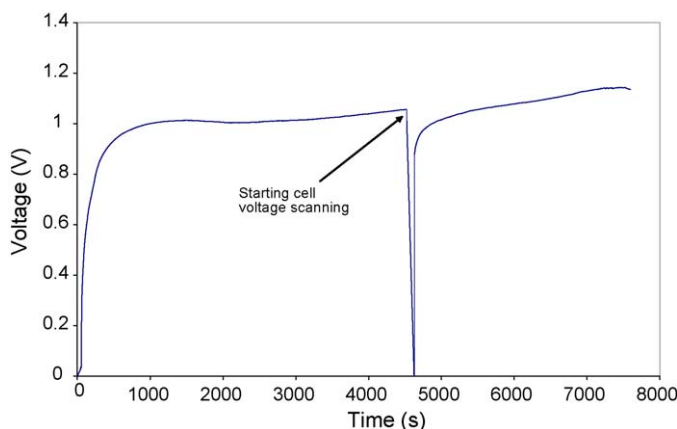


Fig. 6. OCV of the  $\text{H}_2\text{S}$  fuel cell using LA pellet as electrolyte with Mo-Ni-S based anode and NiO cathode at  $600^\circ\text{C}$ .

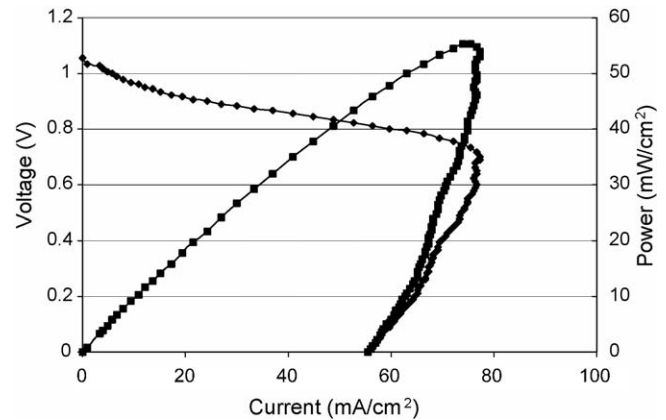


Fig. 7. Electrochemical performance of  $\text{H}_2\text{S}$  fuel cell with Mo-Ni-S based anode and NiO cathode at  $600^\circ\text{C}$  (LA electrolyte thickness: 0.6 mm; scan rate:  $1 \text{ mV s}^{-1}$ ; flow rates— $\text{H}_2\text{S}$ :  $20 \text{ mL min}^{-1}$ ; air:  $2.0 \text{ mL min}^{-1}$ ).

The performance of the fuel cell was determined solely by the proton conductivity of the electrolyte. Proton conductivity determined using the current interruption technique was ca.  $0.01 \text{ S cm}^{-1}$  at  $600^\circ\text{C}$ . Thus the majority of the total ion conductivity as determined using ac-impedance was due to lithium ions rather than protons, and the low power output from the  $\text{H}_2\text{S}$  fuel cell with LA electrolyte was a direct consequence of the low proton conductivity of the electrolyte.

## 4. Conclusions

XRD and XPS results show that  $\text{Li}_2\text{SO}_4$  is reduced to  $\text{Li}_2\text{S}$  under static conditions when heated under  $\text{H}_2\text{S}$ , but not under dynamic  $\text{H}_2\text{S}$  fuel cell operating conditions. Under static conditions, hydrogen produced by pyrolysis of  $\text{H}_2\text{S}$  reduced the electrolyte. Under fuel cell operating conditions  $\text{H}_2$  was converted rapidly to protons, there was no significant concentration of  $\text{H}_2$ , and so reduction of  $\text{Li}_2\text{SO}_4$  by  $\text{H}_2$  did not occur, and the electrolyte was stable during several days operation. The proton conductivity of  $\text{Li}_2\text{SO}_4\text{-Al}_2\text{O}_3$  based electrolyte was ca.  $0.01 \text{ S cm}^{-1}$  at  $600^\circ\text{C}$ . Thus the majority of the total ionic conductivity obtained via ac-impedance testing arose from the conduction of lithium ions. The maximum current and power from a  $\text{H}_2\text{S}$ -air fuel cell with LA as electrolyte,  $\text{MoS}_2\text{-NiS}$  as anode and NiO as cathode were  $80 \text{ mA cm}^{-2}$  and  $56 \text{ mW cm}^{-2}$  at  $600^\circ\text{C}$ . Thus the proton conductivity of  $\text{Li}_2\text{SO}_4$  is too low for its use as electrolyte in practical high temperature pure  $\text{H}_2\text{S}$  fuel cells.

## Acknowledgement

This work is supported by the COURSE program of Alberta Energy Research Institute.

## References

- [1] P. He, M. Liu, J.L. Luo, A.R. Sanger, K.T. Chuang, J. Electrochem. Soc. 149 (2002) A808.

- [2] C. Yates, J. Winnick, *J. Electrochem. Soc.* 146 (1999) 2841.
- [3] N.U. Pujare, K.W. Semkow, A.F. Sammells, *J. Electrochem. Soc.* 134 (1987) 2639.
- [4] H. Iwahara, *Solid State Ionics* 573 (1988) 28.
- [5] T. Norby, *Solid State Ionics* 40–41 (1990) 857.
- [6] H. Iwahara, *Solid State Ionics* 3–4 (1981) 359.
- [7] H. Iwahara, H. Uchida, K. Morimoto, *J. Electrochem. Soc.* 137 (1990) 462.
- [8] T. Hibino, A. Hashimoto, M. Suzuki, M. Sano, *J. Electrochem. Soc.* 149 (2002) A1503.
- [9] K. Katahira, Y. Kohchi, T. Shimura, H. Iwahara, *Solid State Ionics* 138 (2000) 91.
- [10] A. Lundén, *Solid State Ionics* 28–30 (1988) 163.
- [11] R. Kaber, L. Nilsson, N.H. Andersen, A. Lundén, J.O. Thomas, *J. Phys. Condens. Mater.* 4 (1992) 1925.
- [12] A. Lundé, B.-E. Mellander, B. Zhu, *Acta Chem. Scand.* 45 (1991) 981.
- [13] B.-E. Mellander, D. Lazarus, *Phys. Rev. B* 31 (1985) 6801.
- [14] S.W. Tao, Z.L. Zhan, P. Wang, G.Y. Meng, *Solid State Ionics* 116 (1999) 29.
- [15] B. Heed, B. Zhu, B.-E. Mellander, A. Lundén, *Solid State Ionics* 46 (1991) 121.
- [16] B. Zhu, S. Tao, *Solid State Ionics* 127 (2000) 83.
- [17] I. Barin, O. Knacke, *Thermochemical Properties of Inorganic Substances*, Springer, Berlin, 1973.
- [18] N.F. Uvarov, O.P. Shrivastava, E.F. Hairetdinov, *Solid State Ionics* 36 (1989) 39.
- [19] K.T. Chuang, J.L. Luo, G.L. Wei, A.R. Sanger, U.S. Pat. Appl. [20030215697] (2003), Cont.-in-part of U.S. Ser. No. 143,944.
- [20] K.T. Chuang, J.L. Luo, G.L. Wei, A.R. Sanger, PCT Int. Appl. [20030215696] (2003).
- [21] M.A.K.L. Dissanayake, B.-E. Mellander, *Solid State Ionics* 21 (1986) 279.
- [22] S.P. Jiang, Y. Ramprakash, *Solid State Ionics* 122 (1999) 211.
- [23] F.N. Büchi, A. Marek, G. Scherer, *J. Electrochem. Soc.* 142 (1995) 1895.